The frequency of cantilevered double-wall carbon nanotube resonators as a function of outer wall length



2009 J. Phys.: Condens. Matter 21 385301

(http://iopscience.iop.org/0953-8984/21/38/385301)

IOP Publishing Journal of Physics: Condensed Matter

J. Phys.: Condens. Matter **21** (2009) 385301 (6pp) doi:10.1088/0953-8984/21/38/385301

# The frequency of cantilevered double-wall carbon nanotube resonators as a function of outer wall length

**Jeong Won Kang[1], Young Gyu Choi[1], Younghoon Kim[2], Qing Jiang[2], Oh Kuen Kwon[3] and Ho Jung Hwang[4,5]**

[1] Department of Computer Engineering, Chungju National University, Chungju 380-702, Republic of Korea
[2] Department of Mechanical Engineering, University of California, Riverside, CA 92507, USA
[3] Department of Electronic Engineering, Semyung University, Jecheon 390-711, Republic of Korea
[4] School of Electrical and Electronic Engineering, Chung-Ang University, Seoul 156-756, Republic of Korea

E-mail: jwkang@cjnu.ac.kr, jiang@ucr.edu and hjhwang@cau.ac.kr

Received 9 April 2009, in final form 7 August 2009
Published 24 August 2009
Online at stacks.iop.org/JPhysCM/21/385301

**Abstract**

Analysis of vibrational characteristics of cantilevered double-walled carbon nanotube (DWCNT) resonators is carried out based on classical molecular dynamics simulation. Vibrational frequencies of DWCNTs are less than those of single-walled carbon nanotubes (SWCNTs) with the same length and the same diameter because of van der Waals intertube interaction. For DWCNTs with short outer walls, the resonance frequency initially increases with increasing outer nanotube length and then decreases after a peak, and thus the result can be modeled by a Gaussian distribution. The frequency of DWCNT resonators with short outer walls is a maximum when the length of the outer wall is about 72.5% of the length of the inner wall.

(Some figures in this article are in colour only in the electronic version)

## 1. Introduction

Resonators are widely used as key components in signal processing systems [1], and reducing the size of a resonator enhances its resonant frequency and reduces its energy consumption [2]. The higher resonant frequency implies that in general the sensor can have a higher sensitivity [3]. The mechanical quality factor also plays a very important role in determining the sensitivity of nanoelectromechanical system based devices. For wireless communications, higher-frequency resonators enable the production of higher-frequency filters, oscillators, and mixers [1]. The advancement of high-frequency nanoelectromechanical systems is resulting in a diversity of new applications including mechanical mass or charge detectors [4, 5] and nanodevices for high-frequency signal processing [6] and biological imaging [7].

Recently, some researchers have considered the potential applications for carbon nanotubes (CNTs) as resonators [8] and oscillators [9]. For example, the vibrational properties of nanotubes have been studied, and the amplitude of thermal vibrations of cantilevered nanotubes has been used to predict their Young's modulus [10–12]. CNTs exhibit appealing properties, such as an extremely high in-plane elastic modulus and thermal conductivity. The combination of these properties and the nanometer-scale, perfect atomic structure implies that CNTs have potential applications in nanoelectromechanical systems, as components of high-frequency oscillators for sensing and signal processing applications [2–4]. For example, Poncharal *et al* [4] demonstrated how to exploit the resonance of a cantilevered CNT to estimate the mass of an attached carbonaceous particle as light as 30 fg, inside a transmission electron microscope. Recently, Jensen *et al* [3] demonstrated a room-temperature, CNT-based nanomechanical resonator with

[5] Author to whom any correspondence should be addressed.

 

atomic mass resolution, which is based on a nanotube radio receiver design [13]. Chiu *et al* [14] addressed atomic-scale mass sensors using suspended CNT resonators.

Computer simulations have advanced this field and helped reveal the potential of CNT devices in future technologies. Molecular dynamics (MD) has often been used to study and predict the performance of nanoscale machine components. Li and Chou [2] investigated cantilevered SWCNT resonators using molecular mechanics simulations. Jiang *et al* [15] studied the energy dissipation of cantilevered singe-walled CNT oscillators using classical MD simulations. A DWCNT with a short outer wall can be fabricated using a method for thinning and opening of the DWCNT based on oxidation with carbon dioxide [16], and a method for burning of the outer wall based on an electric current [17]. So, cantilevered DWCNT resonators with short outer walls can be considered as alternative high-frequency resonators. Therefore, in this research, we explore the potential of DWCNTs with short outer walls as nanoresonators, using classical MD methods. We demonstrate that the fundamental frequencies of DWCNT resonators can be estimated by a Gaussian distribution, as a function of the outer wall length.

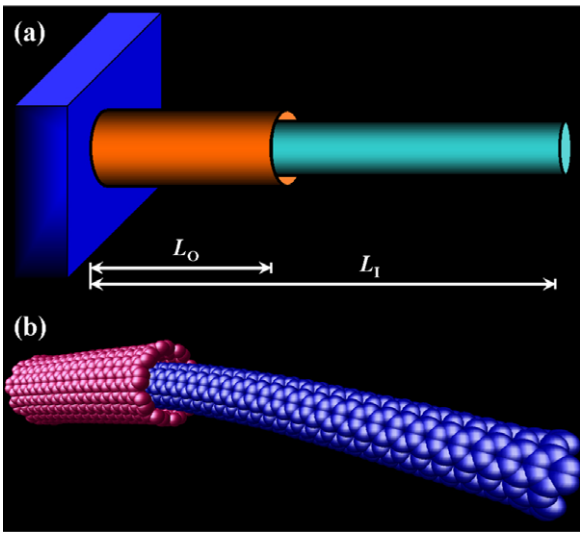


**Figure 1.** (a) Simple schematics of the cantilevered DWCNT resonator with short outer wall. The lengths of the inner and outer walls are denoted by $L_I$ and $L_O$, respectively. (b) The atomic structure of the cantilevered DWCNT resonator with short outer wall in the simulation.

## 2. Simulation methods and structures

In order to investigate cantilevered DWCNT resonators, we used classical MD methods to model the oscillation behavior of DWCNTs. Interactions between carbon atoms that form covalent bonds on CNTs were modeled using the Tersoff–Brenner potential [18, 19], which has been extensively applied to carbon systems [20] and has provided the experimental effectiveness of the simulation results [21]. The long range interactions of carbon were characterized using the Lennard-Jones 12–6 (LJ12–6) potential, based on the parameters obtained by Ulbricht *et al* [22]. In this work, the respective parameters for the LJ12–6 potential were $\varepsilon_{\text{carbon}} = 2.4038 \times 10^{-3}$ eV and $\sigma_{\text{carbon}} = 3.37$ Å. The cutoff distance of the LJ12–6 potential was 10 Å. The MD methods utilized in our previous works [23–26] were implemented using the velocity Verlet algorithm, a Gunsteren–Berendsen thermostat to control the temperature, and neighbor lists to improve the computing performance. The MD time step was $5 \times 10^{-4}$ ps. We assigned the initial atomic velocities with the Maxwell distribution, and the magnitudes were adjusted in order to fit the temperature of the system. In all the MD simulations, the temperature was set to 1 K.

Figure 1(a) shows the simple schematics of the cantilevered DWCNT resonator with the short outer wall. The lengths of the inner and outer walls are denoted by $L_I$ and $L_O$, respectively. Figure 1(b) shows the atomic structure of the cantilevered DWCNT resonator with the short outer wall in the simulation. The left-hand ends of both walls were fixed during the classical MD simulations. The length ($L_I$) of the inner (5, 5) CNT was approximately 50, 75, or 100 Å, and the lengths ($L_O$) of the outer (10, 10) CNTs were changed by 10 Å. In order to obtain the resonant frequencies, we performed MD simulations under an external force of 0.001 eV Å$^{-1}$/atom along the transverse direction for initial 2.5 ps. Upon the removal of the bending force, the CNT resonators were left to oscillate freely. The fundamental resonance frequencies ($f$) were analyzed by using the fast Fourier transform (FFT), based on data sampled at 0.05 ps.

## 3. Results and discussion

Figures 2(a)–(c) show the amplitude spectra of different outer wall lengths ($L_O$) for $L_I = 50$, 75, and 100 Å, respectively. It was explicitly found that the primary peaks corresponding to the fundamental frequencies vary with increasing $L_O$. Figure 3(a) shows the fundamental frequencies as a function of $L_O/L_I$, for $L_I = 50$, 75, and 100 Å. As the $L_O$ increases, the resonance frequency increases initially, and decreases after reaching a peak. This feature is found in all three cases; so we can state that the fundamental frequencies of DWCNT resonators with short outer walls explicitly depend on the length of the outer wall. The frequency ranges covered by DWCNT resonators with short outer walls are 60–128, 29–64, and 16–38 GHz, for $L_I = 50$, 75, and 100 Å, respectively. The differences between the maximum and minimum frequencies are 68, 35, and 16 GHz, for $L_I = 50$, 75, and 100 Å, respectively. Therefore, DWCNT resonators are considered to have a large operating frequency range, as long as the length of their inner walls is short.

For easy comparison, the fundamental frequencies of DWCNT resonators with short outer walls are divided by the fundamental frequencies of simple DWCNT resonators. Figure 3(b) shows the plot of $f/f_{\text{DW}}$ as a function of $L_O/L_I$, for $L_I = 50$, 75, and 100 Å, where $f_{\text{DW}}$ is the fundamental frequency of a (5, 5)(10, 10) DWCNT with a length of $L_I$. The maximum value of $f/f_{\text{DW}}$ increases as the length of the inner wall, $L_I$, increases. The values of $f/f_{\text{DW}}$ have ranges of 0.5–1.2, 0.5–1.3, and 0.5–1.34, for $L_I = 50$, 75, and

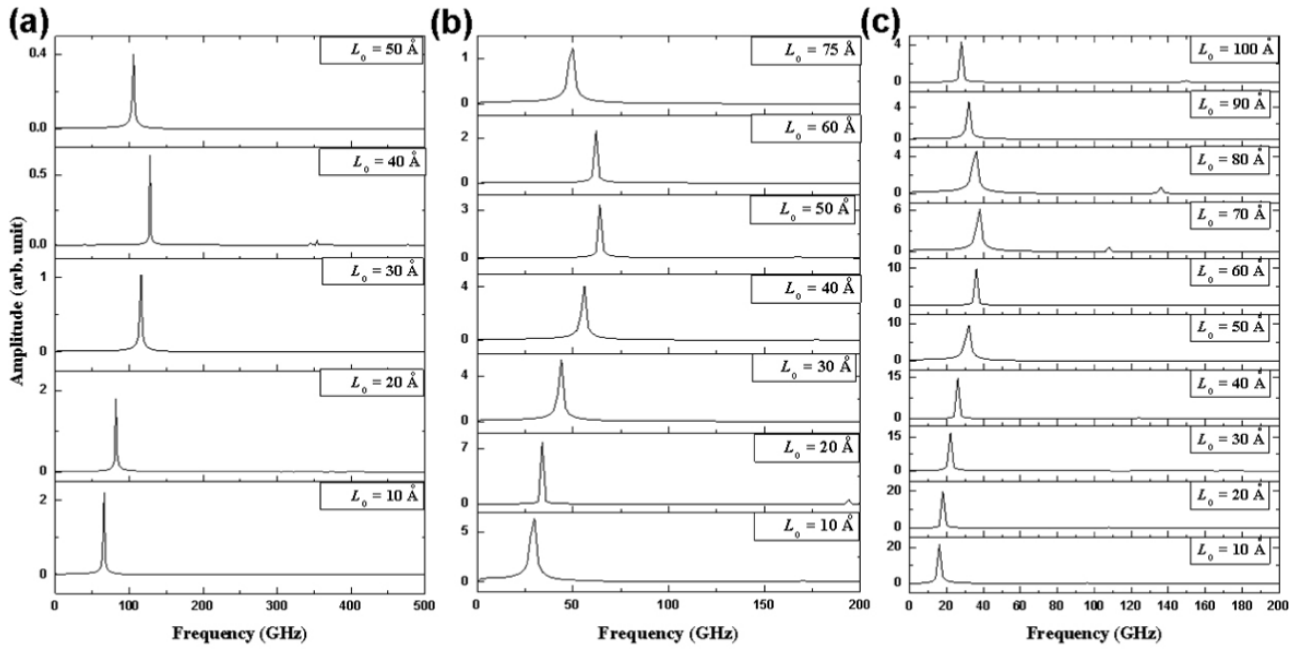


**Figure 2.** Spectra for different outer wall lengths ($L_O$) when $L_I$ is (a) 50, (b) 75, and (c) 100 Å.

100 Å, respectively. These results imply that the frequency of DWCNT resonators with short outer walls is enhanced relative to those with longer inner walls.

We also investigate the fundamental frequencies of DWCNT resonators with short outer walls, which are normalized by the corresponding maximum frequency ($f_{MAX}$). Figure 3(c) shows the plots of $f/f_{MAX}$ as a function of $L_O/L_I$ for $L_I = 50$, 75, and 100 Å. The $f/f_{MAX}$ versus $L_O/L_I$ plots can be regressed by a Gaussian distribution function with mean $\mu = 0.725$ and variance $\sigma = 0.294$, as shown in figure 3(c). Such a Gaussian distribution implies that the frequency of the DWCNT resonators with short outer walls is a maximum when the length of the outer wall is about 72.5% of the length of the inner wall. This property implies that there is a high potential for DWCNT resonators with short outer walls to have engineering applications. If the length of the outer wall can be controlled independently of the inner wall, various frequency devices can be fabricated from a single type of DWCNT with walls of equal length.

Figure 4 shows the fundamental resonance frequency as a function of the length of the (5, 5) SWCNT, (10, 10) SWCNT, and (5, 5)(10, 10) DWCNT. We also plot the data from figure 3(a), to compare simple SWCNT or DWCNT resonators to DWCNT resonators with short outer walls. The DWCNT resonators with short outer walls can have wider frequency ranges than those of the simple SWCNT or DWCNT resonators. Li and Chou [2] predicted the fundamental frequencies of cantilevered SWCNTs using the molecular structural mechanics method. They solved the equation of motion for the problem of free vibration of an undamped structure. So, the frequency range obtained from their results is higher than that obtained from our MD simulations. However, the frequency as a function of length obtained from our MD simulations is in good agreement with their previous work.

In figure 4, the resonance frequencies of the SWCNT (10, 10) are higher than those of DWCNT (10, 10)(5, 5). Conventional wisdom may suggest that DWCNT (10, 10)(5, 5) should be strengthened more than SWCNT (10, 10) by inserting SWCNT (5, 5) into it. The strengthened beam structure DWCNT (10, 10)(5, 5) might have a higher resonance frequency than the hollow beam structure SWCNT (10, 10). However, figure 4 shows exactly the opposite except for very short CNTs. This is because the vibrational properties in the cases of DWCNTs are largely affected by the interwall interactions due to the vibrational deflections of the inner and outer nanotubes. Natsuki *et al* [27], who studied the vibration characteristics of both-side-clamped DWCNTs, found that the SWCNTs have larger vibrational frequencies than the DWCNTs increased by at least 30%. The vibrational frequencies of DWCNTs were between the vibrational frequencies of the inner and outer nanotubes. They discussed that the characteristic frequencies in the cases of DWCNTs are greatly affected by the vibrational deflection of the inner and outer nanotubes. Their results for the bridge-type DWCNT resonators can give important information for our results for the cantilevered-type DWCNT resonators. In this work, the vibrational frequencies of the DWCNTs were about 15% less than those of the SWCNTs with same diameter. The value of 15% in this work is less than the value of 30% in the previous work [27]. However, the difference does not imply any inconsistency between the two works. In this work, we considered one-side-clamped DWCNT resonators whereas Natsuki *et al* [27] considered both-side-clamped DWCNT resonators. When the outer wall length is the same as the inner wall length, the vibrational frequencies for the outer walls are higher than those for the inner walls. Therefore, slowly deflective inner walls can affect the deflective vibration of outer walls and so such noncoaxial intertube vibration phenomena

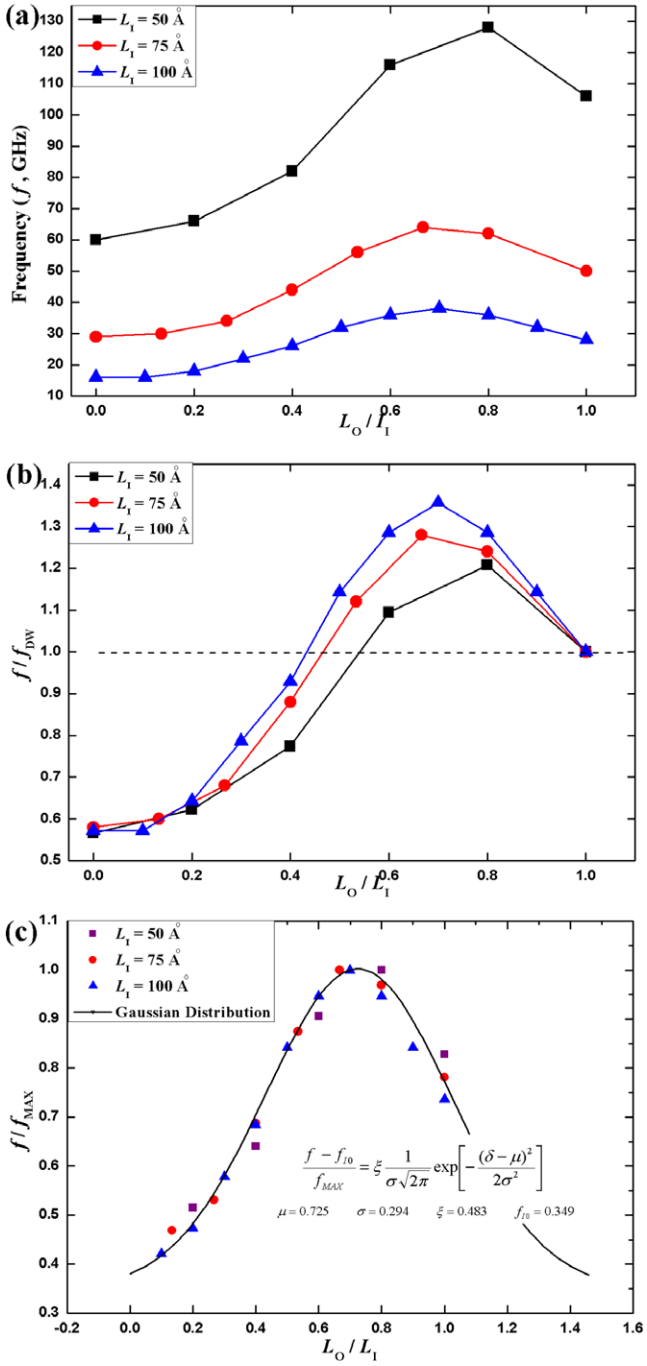


**Figure 3.** (a) Fundamental frequencies as a function of $L_O/L_I$, for $L_I = 50$, 75, and 100 Å. (b) Plot of $f/f_{DW}$ as a function of $L_O/L_I$ for $L_I = 50$, 75, and 100 Å. (c) Plot of $f/f_{MAX}$ as a function of $L_O/L_I$ for $L_I = 50$, 75, and 100 Å.

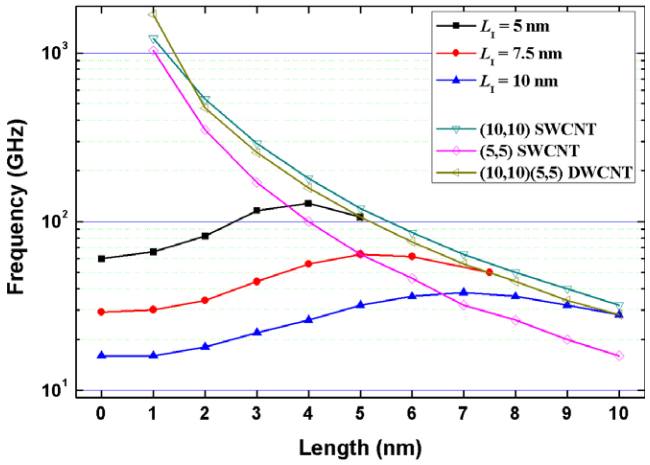


**Figure 4.** Fundamental frequencies as a function of the length of the (5, 5) SWCNT, (10, 10) SWCNT, and (5, 5)(10, 10) DWCNT and as a function of $L_O$ for $L_I = 50$, 75, and 100 Å.

cause the vibrational frequencies of DWCNTs to be less than those of SWCNTs with the same length and the same diameter. The interaction between the inner and outer nanotubes for DWCNTs is considered to be coupled together through the vdW force.

In our MD simulations, the left-hand ends of both the inner and outer walls were fixed, whereas the other ends were free. The right free end of the outer wall can be considered as another boundary of the inner wall, and thus the semi-free boundary condition due to the free end of the outer wall is very important for understanding the vibrations of the cantilevered DWCNT resonator. As the length of the outer wall that covers the inner wall increases, the distance from the free end of the outer wall to the free end of the inner wall decreases. So, such a decrease results in an increase of the fundamental resonance frequency. However, as the length of the outer wall becomes increasingly longer, the un-covered inner wall length becomes shorter. In that case, the impact of the semi-free boundary becomes increasingly smaller. This is found by the decrease of the fundamental resonant frequency after the peak, as shown in figure 3. In this work, peak frequencies are approximately equal to the fundamental frequencies of a (5, 5)(10, 10) DWCNT with a length of $0.85L_I$ ($0.8L_I$–$0.89L_I$).

Our finding that the cantilevered DWCNT resonator has a slightly lower fundamental frequency than the corresponding SWCNT resonator is very important. To obtain more information on whether this phenomena is primarily due to intertube interactions, further work should include various MD simulations for different intertube spacings. This work implies the potential of an alternative application of DWCNTs, as ultrahigh-frequency nanomechanical resonators controlled by the outer wall length. Such ultrahigh-frequency nanomechanical resonators will facilitate the development of fast scanning probe microscopes, magnetic resonant force microscopes, and even mechanical supercomputers, ultrahigh-frequency tuners, and nanodevices for high-frequency signal processing and biological imaging. When the length of the outer wall can be controlled, various resonators with different frequencies can be fabricated from several DWCNTs with walls of equal length.

In this work, we used the (5, 5)(10, 10) DWCNT with the interwall space of 3.4 Å. However, the interwall spacing of DWCNTs ranges from 3.0 to 5.4 Å in experiments [28] and from 3.3 to 3.5 Å in *ab initio* calculations with four different combinations of armchair/zigzag tubes [29]. Recently, Liu *et al* [30] investigated the transport properties of the chirality-resolved DWCNTs for all four types of DWCNTs, which

can be categorized as metallic (M)/semiconducting (S), M/M, S/S, and S/M. The transport characteristics of DWCNTs could be directly correlated with their indices. Their results imply that DWCNT resonators with different chiral indices can have different performances by the direct interwall correlations because electron correlations in DWCNT resonators with different chiral indices affect the properties of the mechanical vibrations. Therefore, in further work we will present a systematical investigation via MD simulation for various DWCNTs with different chiral indices. For cantilevered resonators composed of multi-walled CNTs, since a frequency change can be induced by an interwall length difference, results for multi-walled CNTs will be included in further work. We anticipate confirmation of these phenomena by experiments. Further work should include MD simulations carried out at a range of temperature substantially higher than the 1 K values in the present work to consider thermal dissipation because experiments are most likely to be conducted at temperatures much larger than 1 K. One can expect that the $Q$-factor will be greatly decreased by increasing temperature as in the study on a cantilevered CNT beam oscillator in the previous work by Jiang *et al* [15].

## 4. Summary

In summary, we used classical molecular dynamics simulations to investigate ultrahigh-frequency nanomechanical resonators, which are based on DWCNTs with short outer walls. When the length of the inner wall was constant, the resonance frequency increased and then decreased after the peak, as a function of the length of the outer wall. Thus this trend can be modeled by a Gaussian distribution function. The frequency of the DWCNT resonators with short outer walls was a maximum when the length of the outer wall was about 72.5% of the length of the inner wall. If the length of the outer wall can be controlled independently of the inner wall, various frequency devices can be fabricated from a single type of DWCNT with walls of equal length. Based on the difference between the fundamental frequencies of both SWCNTs and DWCNTs with a given length, the frequency range of a DWCNT resonator with a short outer wall can be enhanced by increasing the length of the inner wall. The characteristics of ultrahigh-frequency nanomechanical resonators fabricated using DWCNTs with short outer walls should be intensively investigated in further works, especially the energy dissipation, damping factor, noise, etc.

## References


[1] De Los Santos H J 1999 *Introduction to Microelectromechanical Microwave Systems* (London: Artech House Publishers)

[2] Li C and Chou T-W 2003 Single-walled carbon nanotubes as ultrahigh frequency nanomechanical resonators *Phys. Rev.* B **68** 073405

[3] Jensen K, Kim K and Zettl A 2008 An atomic-resolution nanomechanical mass sensor *Nat. Nanotechnol.* **3** 533–7

[4] Poncharal P, Wang Z L, Ugarte D and de Heer W A 1999 A carbon nanotube field-emission electron source *Science* **283** 1513–6

[5] Cleland A N and Roukes M L 1998 A nanometre-scale mechanical electrometer *Nature* **392** 160–2

[6] Erbe A and Blick R H 2002 Silicon-on-insulator based nanoresonators for mechanical mixing at radio frequencies *IEEE Trans. Ultrason. Ferroelectr. Freq. Control* **49** 1114–7

[7] Barrett T A, Miers C R, Sommer H A, Mochizuki K and Markert J T 1998 Design and construction of a sensitive nuclear magnetic resonance force microscope *J. Appl. Phys.* **83** 6235–7

[8] Sazonova V, Yaish Y, Ustunel H, Roundy D, Arias T A and McEuen P L 2004 A tunable carbon nanotube electromechanical oscillator *Nature* **431** 284–7

[9] Zheng Q and Jiang Q 2002 Multiwalled carbon nanotubes as gigahertz oscillators *Phys. Rev. Lett.* **88** 045503

[10] Treacy M M J, Ebbesen T W and Gibson T M 1996 Exceptionally high Young's modulus observed for individual carbon nanotubes *Nature* **381** 680–7

[11] Krishnan A, Dujardin E, Ebbesen T W, Yianilos P N and Treacy M M J 1998 Young's modulus of single-walled nanotubes *Phys. Rev.* B **58** 14013–9

[12] Chopra N G and Zettl A 1998 Site-selective radiation damage of collapsed carbon nanotubes *Solid State Commun.* **105** 297–300

[13] Jensen K, Weldon J, Garcia H and Zettl A 2007 Nanotube radio *Nano Lett.* **7** 3508–11

[14] Chiu H-Y, Hung P, Postma C H W and Bockrath M 2008 Atomic-scale mass sensing using carbon nanotube resonators *Nano Lett.* **8** 4342–6

[15] Jiang H, Yu M-F, Liou B and Huang Y 2004 Intrinsic energy loss mechanisms in a cantilevered carbon nanotube beam oscillator *Phys. Rev. Lett.* **93** 185501

[16] Tsang S C, Harris P J F and Green M L H 1993 Thinning and opening of carbon nanotubes by oxidation using carbon dioxide *Nature* **362** 520–2

[17] Collins P G, Hersam M, Arnold M, Martel R and Avouris P 2001 Current saturation and electrical breakdown in multiwalled carbon nanotubes *Phys. Rev. Lett.* **86** 3128–31

[18] Tersoff J 1989 Modeling solid-state chemistry: interatomic potentials for multicomponent systems *Phys. Rev.* B **39** 5566–8

[19] Brenner D W 1990 Empirical potential for hydrocarbons for use in simulating the chemical vapor deposition of diamond films *Phys. Rev.* B **42** 9458–71

[20] Li C, Thostenson E T and Chou T-W 2008 Sensors and actuators based on carbon nanotubes and their composites: a review *Compos. Sci. Technol.* **68** 1227–49

[21] Sinnott S B and Andrews R 2001 Carbon nanotubes: synthesis, properties, and applications *Crit. Rev. Solid State Mater. Sci.* **26** 145–249

[22] Ulbricht H, Moos G and Hertel T 2003 Interaction of $C_{60}$ with carbon nanotubes and graphite *Phys. Rev. Lett.* **90** 095501

[23] Kang J W and Jiang Q 2007 Electrostatically telescoping nanotube nonvolatile memory device *Nanotechnology* **18** 095705

[24] Kang J W and Lee J H 2008 Frequency characteristics of triple-walled carbon nanotube gigahertz devices *Nanotechnology* **19** 285704

[25] Kang J W, Kwon O K and Lee J H 2008 Multi-walled carbon nanotube oscillators as multi-frequency generators for nano embedded systems *J. Comput. Theor. Nanosci.* **5** 290–3

[26] Kang J W, Lee J H, Kim K-S and Choi Y G 2009 Molecular dynamics simulation study on capacitive nano-accelerometers based on telescoping carbon nanotubes *Modelling Simul. Mater. Sci. Eng.* **17** 025011

[27] Natsuki T, Ni Q-Q and Endo M 2008 Analysis of the vibration characteristics of double-walled carbon nanotubes *Carbon* **46** 1570–3

[28] Guisca C E, Tison Y, Stolojan V, Borowiak-Palen E and Silva S R P 2007 Inner-tube chirality determination for double-walled carbon nanotubes by scanning tunneling microscopy *Nano Lett.* **7** 1232–9

[29] Lair S L, Herndon W C and Murr L E 2008 Stability comparison of simulated double-walled carbon nanotube structures *Carbon* **46** 2083–95

[30] Liu K, Wang W, Xu Z, Bai X, Wang E, Yao Y, Zhang J and Liu Z 2009 Chirality-dependent transport properties of double-walled nanotubes measured *in situ* on their field-effect transistors *J. Am. Chem. Soc.* **131** 62–3